

Self-Assembly of a Series of Extended Architectures Based on Polyoxometalate Clusters and Silver Coordination Complexes

Haiyan An, Yanguang Li, Enbo Wang,* Dongrong Xiao, Chunyan Sun, and Lin Xu

Institute of Polyoxometalate Chemistry, Department of Chemistry, Northeast Normal University, Changchun 130024, PRC

Received April 26, 2005

Three unusual compounds based on polyoxometalate building blocks, $[(\text{H}_2\text{O})_5\text{Na}_2(\text{C}_6\text{NO}_2\text{H}_4)(\text{C}_6\text{NO}_2\text{H}_5)_3\text{Ag}_2][\text{Ag}_2\text{-IMo}_6\text{O}_{24}(\text{H}_2\text{O})_4] \cdot 6.25\text{H}_2\text{O}$ (**1**), $[(\text{H}_2\text{O})_4\text{Na}_2(\text{C}_6\text{NO}_2\text{H}_5)_6\text{Ag}_3][\text{IMo}_6\text{O}_{24}] \cdot 6\text{H}_2\text{O}$ (**2**), and $(\text{C}_6\text{NO}_2\text{H}_6)_2[(\text{C}_6\text{NO}_2\text{H}_5)_2\text{Ag}][\text{Cr}(\text{OH})_6\text{Mo}_6\text{O}_{18}] \cdot 4\text{H}_2\text{O}$ (**3**), have been synthesized and characterized by elemental analysis; IR, XPS, and ESR spectroscopy; TG analysis; and single-crystal X-ray diffraction. Compound **1** is constructed from the cationic two-dimensional (2D) coordination polymer sheets which are constituted of $[(\text{H}_2\text{O})_5\text{Na}_2(\text{C}_6\text{NO}_2\text{H}_4)(\text{C}_6\text{NO}_2\text{H}_5)_3\text{Ag}_2]^{3+}$ and anionic $[\text{Ag}_2\text{IMo}_6\text{O}_{24}(\text{H}_2\text{O})_4]^{3-}$ chains as pillars, forming a three-dimensional (3D) supramolecular framework via weak Ag–O interactions. Compound **2** is composed of the well-defined $[\text{IMo}_6\text{O}_{24}]^{5-}$ building blocks, which are linked through trinuclear Ag-pyridine-3-carboxylic acid, $[(\text{C}_6\text{NO}_2\text{H}_5)_6\text{Ag}_3]^{3+}$, fragments into a one-dimensional (1D) hybrid chain; adjacent chains are further connected by sodium cations to yield a novel 2D network. Compound **3** has a 1D chainlike structure constructed from $[\text{Cr}(\text{OH})_6\text{Mo}_6\text{O}_{18}]^{3-}$ building blocks and Ag-pyridine-4-carboxylic acid coordination units. The crystal data for these compounds are the following: **1**, triclinic, $P\bar{1}$, $a = 13.280(3) \text{ \AA}$, $b = 13.641(3) \text{ \AA}$, $c = 16.356(3) \text{ \AA}$, $\alpha = 89.68(3)^\circ$, $\beta = 88.31(3)^\circ$, $\gamma = 75.87(3)^\circ$, $Z = 2$; **2**, triclinic, $P\bar{1}$, $a = 11.978(2) \text{ \AA}$, $b = 12.008(2) \text{ \AA}$, $c = 13.607(3) \text{ \AA}$, $\alpha = 116.14(3)^\circ$, $\beta = 108.85(3)^\circ$, $\gamma = 93.86(3)^\circ$, $Z = 1$; **3**, triclinic, $P\bar{1}$, $a = 10.458(2) \text{ \AA}$, $b = 10.644(2) \text{ \AA}$, $c = 12.295(3) \text{ \AA}$, $\alpha = 97.40(3)^\circ$, $\beta = 112.38(3)^\circ$, $\gamma = 113.59(3)^\circ$, $Z = 1$.

Introduction

Polyoxometalates (POMs), as early transition-metal oxide clusters, bear many properties that make them attractive for applications in catalysis, separation, imaging, materials science, and medicine.^{1–3} Because of the remarkable features of metal oxide surfaces and their diversities in geometric topology, there has recently been an increasing interest in

the assembly of polyoxometalate clusters into extended inorganic or hybrid inorganic–organic solids.^{4–6} It is especially fascinating when new types of polyoxometalates are employed as the building blocks to construct extended solid frameworks in appropriate ways.⁷ To date, several extended high-dimensional assemblies based on well-defined POMs,

* To whom correspondence should be addressed. E-mail: wangenbo@public.cc.jl.cn.

- (1) (a) Pope, M. T. *Heteropoly and Isopoly Oxometalates*; Springer: Berlin, 1983. (b) Anderson, J. S. *Nature* **1937**, *140*, 850. (c) Evans, H. T., Jr. *J. Am. Chem. Soc.* **1948**, *70*, 1291.
- (2) (a) Hill, C. L.; McCartha, C. M. P. *Coord. Chem. Rev.* **1995**, *143*, 407. (b) Hill, C. L. *Chem. Rev.* **1998**, *98*, 1. (c) Kortz, U.; Hamzeh, S. S.; Nasser, N. A. *Chem.–Eur. J.* **2003**, *9*, 2945. (d) Bi, L. H.; Reicke, M.; Kortz, U.; Keita, B.; Nadjo, L.; Clark, R. J. *Inorg. Chem.* **2004**, *43*, 3915. (e) Xu, B. B.; Peng, Z. H.; Wei, Y. G.; Powell, D. R. *Chem. Commun.* **2003**, 2562.
- (3) (a) Müller, A.; Shah, S. Q. N.; Bögge, H.; Schmidtman, M. *Nature* **1999**, *397*, 48. (b) Cronin, L.; Beugholt, C.; Krickemeyer, E.; Schmidtman, M.; Bögge, H.; Kögerler, P.; Luong, T. K. K.; Müller, A. *Angew. Chem., Int. Ed.* **2002**, *41*, 2805. (c) Fukaya, K.; Yamase, T. *Angew. Chem., Int. Ed.* **2003**, *42*, 654. (d) Fang, X. K.; Anderson, T. M.; Benelli, C.; Hill, C. L. *Chem.–Eur. J.* **2005**, *11*, 712. (e) Müller, A.; Kögerler, P.; Kuhlmann, C. *Chem. Commun.* **1999**, 1347.

- (4) (a) Sadakane, M.; Dickman, M. H.; Pope, M. T. *Angew. Chem., Int. Ed.* **2000**, *39*, 2914. (b) Kin, K. C.; Pope, M. T. *J. Am. Chem. Soc.* **1999**, *121*, 8512. (c) Wu, C. D.; Lu, C. Z.; Zhuang, H. H.; Huang, J. S. *J. Am. Chem. Soc.* **2002**, *124*, 3836. (d) Honma, N.; Kusaka, K.; Ozeki, T. *Chem. Commun.* **2002**, 2896.
- (5) (a) Coronado, E.; Galán-Mascarós, J. R.; Giménez-Saiz, C.; Gómez-García, C. J.; Triki, S. *J. Am. Chem. Soc.* **1998**, *120*, 4671. (b) Krebs, B.; Loose, I.; Bösing, M.; Nöh, A.; Doste, E. *C. R. Acad. Sci., Ser. II: Chim.* **1998**, 351. (c) Zhang, J. J.; Sheng, T. L.; Xia, S. Q.; Leibelng, G.; Meyer, F.; Hu, S. M.; Fu, R. B.; Xiang, S. C.; Wu, X. T. *Inorg. Chem.* **2004**, *43*, 5472.
- (6) (a) Zheng, S. L.; Yang, J. H.; Yu, X. L.; Chen, X. M.; Wong, W. T. *Inorg. Chem.* **2004**, *43*, 830. (b) Zhang, L. R.; Shi, Z.; Yang, G. Y.; Chen, X. M.; Feng, S. H.; *J. Chem. Soc., Dalton Trans.* **2000**, 275. (c) Lü, J.; Shen, E. H.; Yuan, M.; Li, Y. G.; Wang, E. B.; Hu, C. W.; Xu, L.; Peng, J. *Inorg. Chem.* **2003**, *42*, 6956.
- (7) (a) Nyman, M.; Bonhomme, F.; Alam, T. M.; Rodriguez, M. A.; Cherry, B. R.; Krumhansl, J. L.; Nenoff, T. M.; Sattler, A. M. *Science* **2002**, *297*, 996. (b) Dolbecq, A.; Mialane, P.; Lisnard, L.; Marrot, J.; Sécherresse, F. *Chem.–Eur. J.* **2003**, *9*, 2914. (c) Cui, X. B.; Xu, J. Q.; Meng, H.; Zheng, S. T.; Yang, G. Y. *Inorg. Chem.* **2004**, *43*, 8005.

such as Keggin,⁸ Wells–Dawson,⁹ and Lindquist-type,¹⁰ or new POM units, spherical vanadium oxides,¹¹ and capped clusters,¹² for instance, have been successfully reported. However, the use of Anderson-type polyoxoanions and their derivatives as inorganic building blocks in this aspect has not been so extensively studied.¹³ It therefore will be of great interest to investigate whether this kind of polyoxometalate and its derivatives can be introduced into high-dimensional frameworks. More recently, successful syntheses of a few polymers^{14,15} based on Anderson-type polyoxoanions and rare-earth cations by our group and other groups further inspired our research ardor for constructing novel architectures from this kind of polyoxoanion by replacement of the linkers from rare-earth cations with other transition-metal cations or complexes.

On the other hand, POM-based extended structures containing silver(I) ions and/or their coordination complexes are comparatively unexplored.¹⁶ This is unexpected for two main reasons: (i) the probable synergistic effect between silver(I) ions and POMs could strongly improve their catalytic selectivity when utilized as catalysts for the oxidation of numerous organic molecules such as alcohols and aldehydes, as compared with that of the POM precursors,^{17,18} and (ii) the silver(I) atom has a labile metal center with versatile coordination properties, generally adopting coordination numbers of 2–6 in covalent complexes, and therefore can become an important choice as the bridging linker in the design of novel POM-based compounds.^{18,19} Furthermore, Anderson-type polyoxometalates have recently been demonstrated as catalysts for the oxidation of vicinal

diols,²⁰ hydrogenolysis, or NO–CO reactions.^{21,22} However, no structural information on silver-linked Anderson-type polyoxometalates has been reported in the literature, although they may possess potential catalytic properties. Taking this into account, our current synthetic strategy is to acquire new extended architectures based on silver(I) ions and Anderson-type polyoxoanions, including A-type and B-type structures. In addition, pyridine-4-carboxylic acid and pyridine-3-carboxylic acid molecules were chosen as the organic components, not only because of their role as good monodentate and bridging ligands and because of the requirement for acid reaction conditions but also to further understand the effect of the different introduced organic molecules on the whole framework.

When we chose the A-type Anderson cluster $[\text{IMo}_6\text{O}_{24}]^{5-}$ as the building block and the pyridine-4-carboxylic acid/pyridine-3-carboxylic acid molecule as the organic component, two unique compounds were obtained, $[(\text{H}_2\text{O})_5\text{Na}_2(\text{C}_6\text{NO}_2\text{H}_4)(\text{C}_6\text{NO}_2\text{H}_5)_3\text{Ag}_2][\text{Ag}_2\text{IMo}_6\text{O}_{24}(\text{H}_2\text{O})_4] \cdot 6.25\text{H}_2\text{O}$ (**1**) and $[(\text{H}_2\text{O})_4\text{Na}_2(\text{C}_6\text{NO}_2\text{H}_5)_6\text{Ag}_3][\text{IMo}_6\text{O}_{24}] \cdot 6\text{H}_2\text{O}$ (**2**). When the B-type Anderson cluster $[\text{Cr}(\text{OH})_6\text{Mo}_6\text{O}_{18}]^{3-}$ was utilized as the structure motif in the presence of a pyridine-4-carboxylic acid molecule under similar conditions, a structure that differed from the above two was obtained, $(\text{C}_6\text{NO}_2\text{H}_6)_2[(\text{C}_6\text{NO}_2\text{H}_5)_2\text{Ag}][\text{Cr}(\text{OH})_6\text{Mo}_6\text{O}_{18}] \cdot 4\text{H}_2\text{O}$ (**3**). The unique complex **1** is built of a new type of $[\text{IMo}_6\text{O}_{24}(\text{H}_2\text{O})_4]^{5-}$ cluster as the structural motif, which is covalently linked by silver ions to yield unprecedented one-dimensional (1D) chains which further pillar the silver-organic coordination polymer sheets to form a three-dimensional (3D) framework via weak Ag–O interactions, and the free water molecules reside in the frameworks. To the best of our knowledge, compound **1** represents the first example of 3D supramolecular structures containing polyoxometalate chains as pillars. The unique structural character in **1** not only represents a new type of pillaring mode but also indicates that the flexible coordinative behavior of POMs can be effectively used to construct novel 3D pillared structures. Compound **2** is a novel two-dimensional (2D) hybrid network, with the well-characterized $[\text{IMo}_6\text{O}_{24}]^{5-}$ building blocks connected by trinuclear Ag–pyridine-3-carboxylic acid $[(\text{C}_6\text{NO}_2\text{H}_5)_6\text{Ag}_3]^{3+}$ fragments and Na^+ cations in two directions. Compound **3** has a 1D chainlike structure built from alternating $[\text{Cr}(\text{OH})_6\text{Mo}_6\text{O}_{18}]^{3-}$ building blocks and Ag–pyridine-4-carboxylic acid coordination units.

Experimental Section

General Considerations. All chemicals were commercially purchased and used without further purification. $\text{Na}_5[\text{IMo}_6\text{O}_{24}]^{5-}$

- (8) (a) Reinoso, S.; Vitoria, P.; Lezama, L.; Luque, A.; Gutiérrez-Zorrilla, J. M. *Inorg. Chem.* **2003**, *42*, 3709. (b) Lu, Y.; Xu, Y.; Wang, E. B.; Lu, J.; Hu, C. W.; Xu, L. *Cryst. Growth Des.* **2005**, *5*, 257. (c) Bonhomme, F.; Larentzou, J. P.; Alam, T. M.; Maginn, E. J.; Nyman, M. *Inorg. Chem.* **2005**, *44*, 1774.
- (9) (a) Bareyt, S.; Piligkos, S.; Hasenknopf, B.; Gouzerh, P.; Lacôte, E.; Thorimbert, S.; Malacria, M. *Angew. Chem., Int. Ed.* **2003**, *42*, 3404. (b) Niu, J. Y.; Wei, M. L.; Wang, J. P.; Dang, D. B. *Eur. J. Inorg. Chem.* **2004**, 160. (c) Wang, J. P.; Zhao, J. W.; Niu, J. Y. *J. Mol. Struct.* **2004**, *697*, 191.
- (10) Hagrman, P. J.; Hagrman, D.; Zubieta, J. *Angew. Chem., Int. Ed.* **1999**, *38*, 3165.
- (11) (a) Khan, M. I.; Yohannes, E.; Powell, D. *Chem. Commun.* **1999**, 23. (b) Khan, M. I.; Yohannes, E.; Doedens, R. J. *Angew. Chem., Int. Ed.* **1999**, *38*, 1292. (c) Pan, C. L.; Xu, J. Q.; Li, G. H.; Chu, D. Q.; Wang, T. G. *Eur. J. Inorg. Chem.* **2004**, 160.
- (12) (a) Luan, G. Y.; Wang, E. B.; Han, Z. B.; Li, Y. G. *Inorg. Chem. Commun.* **2001**, *4*, 541. (b) Duan, L. M.; Pan, C. L.; Xu, J. Q.; Cui, X. B.; Xie, F. T.; Wang, T. G. *Eur. J. Inorg. Chem.* **2003**, 2578.
- (13) (a) Shivaiah, V.; Nagaraju, M.; Das, S. K. *Inorg. Chem.* **2003**, *42*, 6604. (b) Martin, C.; Lamonier, C.; Fournier, M.; Mentré, O.; Harlé, V.; Guillaume, D.; Payen, E. *Inorg. Chem.* **2004**, *43*, 4636.
- (14) (a) An, H. Y.; Xiao, D. R.; Wang, E. B.; Li, Y. G.; Wang, X. L.; Xu, L. *Eur. J. Inorg. Chem.* **2005**, 854. (b) An, H. Y.; Lan, Y.; Li, Y. G.; Wang, E. B.; Hao, N.; Xiao, D. R.; Duan, L. Y.; Xu, L. *Inorg. Chem. Commun.* **2004**, *7*, 356. (c) An, H. Y.; Wang, E. B.; Xiao, D. R.; Li, Y. G.; Xu, L. *Inorg. Chem. Commun.* **2005**, *8*, 267.
- (15) (a) Drewes, D.; Limanski, E. M.; Krebs, B. *J. Chem. Soc., Dalton Trans.* **2004**, *14*, 2087. (b) Drewes, D.; Limanski, E. M.; Krebs, B. *Eur. J. Inorg. Chem.* **2004**, *24*, 4849. (c) Shivaiah, V.; Reddy, P. V. N.; Cronin, L.; Das, S. K. *J. Chem. Soc., Dalton Trans.* **2002**, 3781.
- (16) Han, Z. G.; Zhao, Y. L.; Peng, J.; Ma, H. Y.; Liu, Q.; Wang, E. B.; Hu, N. H.; Jia, H. J. *Eur. J. Inorg. Chem.* **2005**, *2*, 264.
- (17) Rhule, J. T.; Neiwert, W. A.; Hardcastle, K. I. B.; Do, T.; Hill, C. L. *J. Am. Chem. Soc.* **2001**, *123*, 12101.
- (18) Liu, F. X.; Marchal-Roch, C.; Bouchard, P.; Marrot, J.; Simonato, J. P.; Hervé, G.; Sécheresse, F. *Inorg. Chem.* **2004**, *43*, 2240.

- (19) (a) Bu, X. H.; Chen, W.; Du, M.; Biradha, K.; Wang, W. Z.; Zhang, R. H. *Inorg. Chem.* **2002**, *41*, 437. (b) Yang, J. H.; Zheng, S. L.; Yu, X. L.; Chen, X. M. *Cryst. Growth Des.* **2004**, *4*, 831. (c) Luan, G. Y.; Li, Y. G.; Wang, S. T.; Wang, E. B.; Han, Z. B.; Hu, C. W.; Hu, N. H.; Jia, H. Q. *J. Chem. Soc., Dalton Trans.* **2003**, 233.
- (20) Khenkin, A. M.; Neumann, R. *Adv. Synth. Catal.* **2002**, *344*, 1017.
- (21) (a) Cabelloa, C. I.; Botto, I. L.; Thomas, H. J. *Appl. Catal., A* **2000**, *197*, 79. (b) Martin, C.; Lamonier, C.; Fournier, M.; Mentré, O.; Harlé, V.; Guillaume, D.; Payen, E. *Inorg. Chem.* **2004**, *43*, 4636.
- (22) Kondaries, D. J.; Tomishige, K.; Nagasawa, Y.; Lee, U.; Iwasawa, Y. *J. Mol. Catal. A* **1996**, *111*, 145.

$3\text{H}_2\text{O}^{23}$ and $\text{Na}_3[\text{Cr}(\text{OH})_6\text{Mo}_6\text{O}_{18}] \cdot 8\text{H}_2\text{O}^{24}$ were synthesized according to the literature and characterized by IR spectroscopy and TG analyses. Elemental analyses (C, H, and N) were performed on a Perkin-Elmer 2400 CHN elemental analyzer, and I, Cr, Mo, Ag, and Na were analyzed on a PLASMA-SPEC(I) ICP atomic emission spectrometer. XPS analyses were performed on a VG ESCALABMKII spectrometer with a Mg K α (1253.6 eV) achromatic X-ray source. The vacuum inside the analysis chamber was maintained at 6.2×10^{-6} Pa during the analysis. IR spectra were recorded in the range of 400–4000 cm^{-1} on an Alpha Centaur FT/IR spectrophotometer using KBr pellets. The ESR spectrum was recorded on a Japanese JES-FE3AX spectrometer at room temperature. TG analyses were performed on a Perkin-Elmer TGA7 instrument in flowing N_2 with a heating rate of 10 $^\circ\text{C min}^{-1}$.

Synthesis. $[(\text{H}_2\text{O})_5\text{Na}_2(\text{C}_6\text{NO}_2\text{H}_4)(\text{C}_6\text{NO}_2\text{H}_5)_3\text{Ag}_2][\text{Ag}_2\text{IMo}_6\text{O}_{24}(\text{H}_2\text{O})_4] \cdot 6.25\text{H}_2\text{O}$ (**1**). AgNO_3 (0.085 g, 0.5 mmol) and pyridine-4-carboxylic acid (0.0615 g, 0.5 mmol) were dissolved in 30 mL of hot water. Then, a 30-mL water solution of $\text{Na}_5[\text{IMo}_6\text{O}_{24}] \cdot 3\text{H}_2\text{O}$ (0.6283 g, 0.5 mmol) was added. The mixture was heated for 1 h at 80 $^\circ\text{C}$ and then filtered. The filtrate was kept for 2 weeks at ambient conditions, and then colorless block crystals of **1** were isolated in about 36% yield (based on Ag). Anal. Calcd for $[(\text{H}_2\text{O})_5\text{Na}_2(\text{C}_6\text{NO}_2\text{H}_4)(\text{C}_6\text{NO}_2\text{H}_5)_3\text{Ag}_2][\text{Ag}_2\text{IMo}_6\text{O}_{24}(\text{H}_2\text{O})_4] \cdot 6.25\text{H}_2\text{O}$: I, 5.45; Mo, 24.70; Na, 1.97; Ag, 18.52; C, 12.37; N, 2.40; H, 2.12 (%). Found: I, 5.24; Mo, 24.55; Na, 2.12; Ag, 18.79; C, 12.20; N, 2.65; H, 2.38 (%). FTIR (cm^{-1}): 3528(s), 3452(s), 3351(s), 1963(w), 1714(m), 1607(m), 1548(m), 1413(m), 1390(m), 1337(w), 1301(w), 1232(w), 1215(w), 1092(w), 1029(m), 942(s), 904(vs), 889(s), 858(m), 764(s), 698(vs), 624(s), 563(m), 539(m), 476(m), 417(m).

$[(\text{H}_2\text{O})_4\text{Na}_2(\text{C}_6\text{NO}_2\text{H}_5)_6\text{Ag}_3][\text{IMo}_6\text{O}_{24}] \cdot 6\text{H}_2\text{O}$ (**2**). AgNO_3 (0.085 g, 0.5 mmol) and pyridine-3-carboxylic acid (0.0615 g, 0.5 mmol) were dissolved in 30 mL of hot water. Then, a 30-mL water solution of $\text{Na}_5[\text{IMo}_6\text{O}_{24}] \cdot 3\text{H}_2\text{O}$ (0.6283 g, 0.5 mmol) was added. The mixture was heated for 1 h at 80 $^\circ\text{C}$ and then filtered. The filtrate was kept for 3 weeks at ambient conditions, and then yellow block crystals of **2** were isolated in about 30% yield (based on Ag). Anal. Calcd for $[(\text{H}_2\text{O})_4\text{Na}_2(\text{C}_6\text{NO}_2\text{H}_5)_6\text{Ag}_3][\text{IMo}_6\text{O}_{24}] \cdot 6\text{H}_2\text{O}$: I, 5.34; Mo, 24.24; Na, 1.96; Ag, 13.63; C, 18.19; N, 3.54; H, 2.11 (%). Found: I, 5.45; Mo, 24.13; Na, 1.76; Ag, 13.85; C, 18.04; N, 3.28; H, 2.47 (%). FTIR (cm^{-1}): 3539(s), 3460(s), 3100(m), 3066(m), 3039(m), 2919(m), 2795(m), 2630(m), 2507(m), 2076(w), 1951(w), 1729(s), 1638(m), 1604(s), 1477(w), 1442(w), 1418(w), 1391(w), 1327(m), 1293(s), 1202(w), 1187(w), 1145(w), 1116(w), 1089(w), 1050(w), 1035(w), 941(vs), 905(vs), 813(w), 745(s), 693(vs), 681(vs), 622(vs), 538(w), 494(w), 470(m).

$(\text{C}_6\text{NO}_2\text{H}_6)_2[(\text{C}_6\text{NO}_2\text{H}_5)_2\text{Ag}][\text{Cr}(\text{OH})_6\text{Mo}_6\text{O}_{18}] \cdot 4\text{H}_2\text{O}$ (**3**). AgNO_3 (0.085 g, 0.5 mmol) and pyridine-4-carboxylic acid (0.0615 g, 0.5 mmol) were dissolved in 30 mL of hot water. Then, a 30-mL water solution of $\text{Na}_3[\text{Cr}(\text{OH})_6\text{Mo}_6\text{O}_{18}] \cdot 8\text{H}_2\text{O}$ (0.6155 g, 0.5 mmol) was added. The mixture was heated for 1 h at 80 $^\circ\text{C}$ and then filtered. The filtrate was kept for 1 month at ambient conditions, and pink block crystals of **3** were isolated in about 24% yield (based on Ag). Anal. Calcd for $[(\text{C}_6\text{NO}_2\text{H}_6)_2][(\text{C}_6\text{NO}_2\text{H}_5)_2\text{Ag}][\text{Cr}(\text{OH})_6\text{Mo}_6\text{O}_{18}] \cdot 4\text{H}_2\text{O}$: Cr, 3.07; Mo, 34.02; Ag, 6.37; C, 17.02; N, 3.31; H, 2.13 (%). Found: Cr, 3.27; Mo, 34.19; Ag, 6.11; C, 17.32; N, 3.01; H, 2.03 (%). FTIR (cm^{-1}): 3563(w), 3238(s), 3150(s), 3104(s), 1976(m), 1712(m), 1639(m), 1620(m), 1571(s), 1495(m), 1361(s), 1241(m), 1223(m), 1140(w), 1079(w), 1050(w),

999(w), 942(vs), 922(vs), 907(vs), 886(vs), 852(w), 830(w), 795(w), 767(m), 757(m), 680(m), 642(vs), 561(s), 537(s), 412(s).

X-ray Crystallography. A colorless single crystal of **1** with dimensions of $0.25 \times 0.13 \times 0.11$ mm was fixed to the end of a glass capillary. The data were collected on a Rigaku R-Axis RAPID IP diffractometer with Mo K α ($\lambda = 0.71073$ Å) at 293 K in the range of $2.99^\circ < \theta < 27.48^\circ$. Empirical absorption correction was applied. A total of 28 080 (13 022 unique, $R_{\text{int}} = 0.0381$) reflections were measured ($-14 \leq h \leq 17$, $-17 \leq k \leq 17$, $-21 \leq l \leq 21$). A yellow single crystal of **2** with dimensions of $0.23 \times 0.16 \times 0.12$ mm was fixed to the end of a glass capillary. The data were collected on a Rigaku R-Axis RAPID IP diffractometer with Mo K α ($\lambda = 0.71073$ Å) at 293 K in the range of $3.00^\circ < \theta < 27.48^\circ$. Empirical absorption correction was applied. A total of 15 499 (7239 unique, $R_{\text{int}} = 0.0530$) reflections were measured ($-13 \leq h \leq 15$, $-15 \leq k \leq 15$, $-17 \leq l \leq 16$). A pink single crystal of **3** with dimensions of $0.25 \times 0.20 \times 0.15$ mm was fixed to the end of a glass capillary. The data were collected on a Rigaku R-Axis RAPID IP diffractometer with Mo K α ($\lambda = 0.71073$ Å) at 293 K in the range of $3.27^\circ < \theta < 27.48^\circ$. Empirical absorption correction was applied. A total of 10 692 (4942 unique, $R_{\text{int}} = 0.0401$) reflections were measured ($-13 \leq h \leq 13$, $-13 \leq k \leq 13$, $-15 \leq l \leq 15$).

The structures of **1**, **2**, and **3** were solved by the direct method and refined by the full-matrix least-squares method on F^2 using the SHELXTL-97 software.²⁵ All non-hydrogen atoms in **1**, **2**, and **3** were refined anisotropically. In **1**, only positions of the hydrogen atoms attached to OW3 and OW4 were located from difference maps, and those attached to other water molecules were not located. The hydrogen atoms attached to the nitrogen atoms and the hydrogen atoms attached to the carbon atoms were fixed in ideal positions in **1**. In **2**, the hydrogen atoms attached to the nitrogen atoms and those attached to the carbon atoms were fixed in ideal positions, and the other hydrogen atoms were not located. In **3**, positions of the hydrogen atoms attached to polyoxoanions, those attached to the nitrogen atoms, and those attached to the carbon atoms were located from difference maps, and other hydrogen atoms were not located. A summary of the crystallographic data and structural determination for **1**, **2**, and **3** is provided in Table 1. Bond lengths and angles with standard deviations in parentheses of **1**, **2**, and **3** are listed in Table 2.

The CCDC reference numbers are 268273 for **1**, 268274 for **2**, and 268275 for **3**.

Results and Discussion

Crystal Structure of 1. Single-crystal X-ray structural analysis reveals that the structure of **1** is constructed from the cationic 2D coordination polymer sheets, $[(\text{H}_2\text{O})_5\text{Na}_2(\text{C}_6\text{NO}_2\text{H}_4)(\text{C}_6\text{NO}_2\text{H}_5)_3\text{Ag}_2]^{3+}$, pillared by anionic $[\text{Ag}_2\text{IMo}_6\text{O}_{24}(\text{H}_2\text{O})_4]^{3-}$ chains into a 3D supramolecular channel framework via weak Ag–O interactions with the water molecules residing in it. The basic building block $[\text{IMo}_6\text{O}_{24}(\text{H}_2\text{O})_4]^{5-}$ in **1** is shown in Figure 1. The asymmetric unit in the structure of **1** consists of two crystallographically independent “one-half” $[\text{IMo}_6\text{O}_{24}(\text{H}_2\text{O})_4]^{5-}$ anions, in which both iodine ions (I(1) and I(2)) occupy special positions (see Figure 2). The $[\text{IMo}_6\text{O}_{24}(\text{H}_2\text{O})_4]^{5-}$ cluster is a new type of structural motif, differing from the well-defined Anderson structure,

(23) Filowitz, M.; Ho, R. K. C.; Klemperer, W. G.; Shum, W. *Inorg. Chem.* **1979**, *18*, 93.

(24) Perloff, A. *Inorg. Chem.* **1970**, *9*, 2228.

(25) (a) Sheldrick, G. M. *SHELXL 97: Program for Crystal Structure Refinement*; University of Göttingen: Göttingen, Germany, 1997. (b) Sheldrick, G. M. *SHELXL 97: Program for Crystal Structure Solution*; University of Göttingen: Göttingen, Germany, 1997.

Table 1. Crystal Data and Structure Refinement for Compounds 1–3

	1	2	3
chemical formula	C ₂₄ H _{49.50} Ag ₄ IMo ₆ N ₄ Na ₂ O _{47.25}	C ₃₆ H ₅₀ Ag ₃ IMo ₆ N ₆ Na ₂ O ₄₆	C ₂₄ H ₃₆ AgCrMo ₆ N ₄ O ₃₆
fw	2330.18	2374.95	1692.08
<i>T</i> (K)	293(2)	293(2)	293(2)
λ (Å)	0.71073	0.71073	0.71073
cryst syst	triclinic	triclinic	triclinic
space group	<i>P</i> $\bar{1}$	<i>P</i> $\bar{1}$	<i>P</i> $\bar{1}$
<i>a</i> (Å)	13.280(3)	11.978(2)	10.458(2)
<i>b</i> (Å)	13.641(3)	12.008(2)	10.644(2)
<i>c</i> (Å)	16.356(3)	13.607(3)	12.295(3)
α (deg)	89.68(3)	116.14(3)	97.40(3)
β (deg)	88.31(3)	108.85(3)	112.38(3)
γ (deg)	75.87(3)	93.86(3)	113.59(3)
<i>V</i> (Å ³)	2872.2(10)	1611.4(6)	1094.0(4)
<i>Z</i>	2	1	1
<i>D</i> _c (g/cm ³)	2.691	2.447	2.568
μ (mm ⁻¹)	3.267	2.625	2.458
<i>R</i> _{int}	0.0381	0.0530	0.0401
GOF on <i>F</i> ²	1.020	0.97	1.00
<i>R</i> 1 ^a [<i>I</i> > 2 σ (<i>I</i>)]	0.0427	0.0491	0.0268
w <i>R</i> 2 ^b [<i>I</i> > 2 σ (<i>I</i>)]	0.1129	0.1202	0.0738
<i>R</i> 1 (all data)	0.1030	0.0829	0.0305
w <i>R</i> 2 (all data)	0.1314	0.1377	0.0755
largest diff. peak and hole (e Å ⁻³)	3.031 and -1.284	1.068 and -0.975	0.657 and -0.614

$$^a R1 = \sum |F_o| - |F_c| / \sum |F_o|. \quad ^b wR2 = \sum [w(F_o^2 - F_c^2)^2] / \sum [w(F_o^2)^2]^{1/2}.$$

Table 2. Bond Lengths (Å) and Angles (deg) with Standard Deviations of Compounds 1–3 in Parentheses

Compound 1			
I–Oc	1.858(9)–1.902(11)	Ag(1)–O(17)	2.176(10)
Mo–Ot	1.700(13)–1.728(12)	Ag(1)–O(9)	2.184(10)
Mo–Ot'	1.705(13)–1.725(13)	Ag(1)–O(4)#5	2.571(14)
Mo–Ow	2.409(13)–2.421(12)	Ag(1)–O(22)#6	2.582(14)
Mo–Ob	1.858(11)–1.978(11)	Ag(2)–O(18)	2.167(10)
Mo–Oc	2.222(11)–2.238(10)	Ag(2)–O(8)	2.176(10)
Mo–Oc'	2.222(10)–2.238(10)	Ag(2)–O(10)	2.568(15)
Na(1)–O	2.35(2)–2.724(16)	Ag(2)–O(13)	2.583(14)
Na(2)–O	2.35(2)–2.714(15)	Ag(3)–N(2)	2.130(17)
Ag(4)–N(3)	2.146(16)	Ag(3)–N(1)	2.156(18)
Ag(4)–N(4)	2.158(16)		
O–I–O _{cis}	86.1(5)–93.9(5)	O–Mo–O _{cis}	67.3(3)–108.0(5)
O–I–O _{trans}	180.0	O–Mo–O _{trans}	148.4(4)–163.6(4)
Compound 2			
I–Oc	1.876(5)–1.887(4)	Ag(1)–N(1)	2.178(6)
Mo–Ot	1.709(6)–1.711(5)	Ag(1)–N(2)	2.191(6)
Mo–Ot ₁	1.703(5)–1.711(5)	Ag(1)–O(7)	2.586(5)
Mo–Ot ₂	1.703(5)–1.716(4)	Ag(1)–O(9)	2.631(5)
Mo–Ob	1.916(5)–1.941(5)	Ag(2)–N(3)	2.153(6)
Mo–Oc	2.298(4)–2.359(5)	Na–O	2.364(6)–2.462(7)
O–I–O _{cis}	86.6(2)–93.4(2)	O–Mo–O _{cis}	66.68(16)–106.6(3)
O–I–O _{trans}	180.0	O–Mo–O _{trans}	150.7(2)–162.4(2)
Compound 3			
Cr–Oc	1.9556(18)–1.980(2)	Mo–Oc	2.228(2)–2.327(2)
Mo–Ot	1.698(2)–1.722(2)	Ag(1)–O(7)	2.352(2)
Mo–Ot'	1.720(2)	Ag(1)–O(13)	2.492(3)
Mo–Ob	1.922(2)–1.9657(19)		
O–Cr–O _{cis}	82.45(9)–97.55(9)	O–Mo–O _{cis}	69.92(8)–161.39(10)
O–Cr–O _{trans}	180.0	O–Mo–O _{trans}	150.68(9)–162.4(2)

[IMo₆O₂₄]⁵⁻, in which a central {IO₆} octahedron with six {MoO₆} octahedra surround it in a plane by sharing their edges. In the unique [IMo₆O₂₄(H₂O)₄]⁵⁻ cluster, there is not only edge sharing but also corner sharing between the central {IO₆} octahedron and surrounding {MoO₆} and/or {MoO₅(H₂O)} octahedra, and there also is edge sharing and corner sharing between {MoO₆} and/or {MoO₅(H₂O)} octahedra. Interestingly, four water molecules coordinate to four different Mo atoms to finish the {MoO₅(H₂O)} octahedral environment in each [IMo₆O₂₄(H₂O)₄]⁵⁻ cluster. To the best of our knowledge, this framework has never been described

so far in the chemistry of POMs. According to the way the oxygen atoms are coordinated, six kinds of oxygen atoms exist in the cluster: terminal oxygen Ot, terminal oxygen Ot' linked to Ag⁺, terminal water molecule Ow, double-bridging oxygen Ob, central oxygen Oc, and central oxygen Oc' linked to Ag⁺. Thus, the Mo–O bond lengths fall into six classes: Mo–Ot = 1.700(13)–1.728(12) Å, Mo–Ot' = 1.705(13)–1.725(13) Å, Mo–Ow = 2.409(13)–2.421(12) Å, Mo–Ob = 1.858(11)–1.978(11) Å, Mo–Oc = 2.222(11)–2.238(10) Å, and Mo–Oc' = 2.222(10)–2.238(10) Å. The central I–O distances vary from 1.858(9) to 1.902(11)

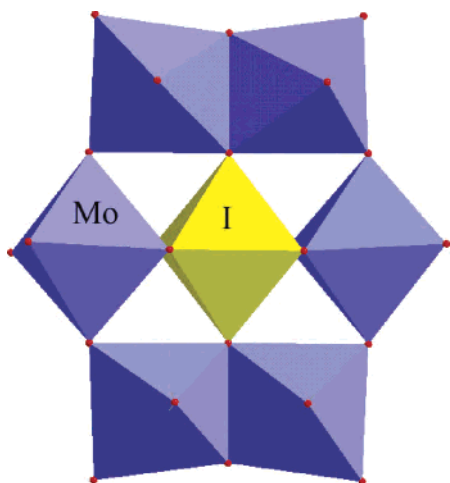


Figure 1. Representation of the polyoxometalate building block in **1**, showing the metal atoms and their coordination polyhedra.

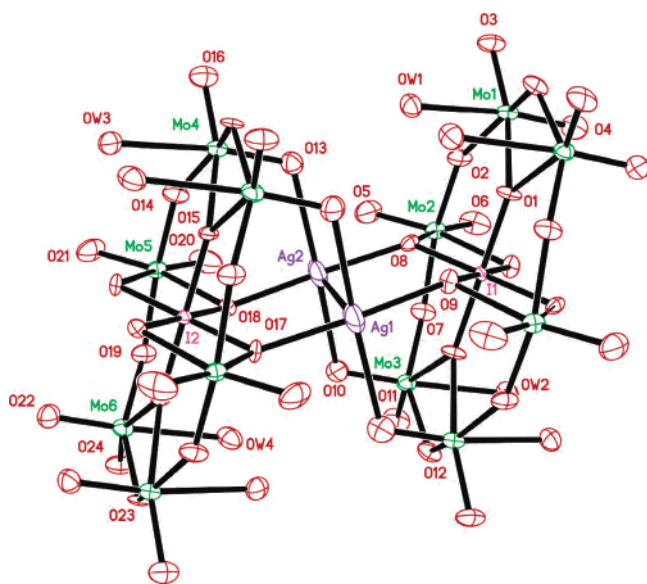


Figure 2. ORTEP drawing of **1** with thermal ellipsoids at 50% probability. Only parts of atoms are labeled, and metal-organic moieties have been omitted for clarity.

Å. The bond angles of O–I–O_{cis} range from 86.1(5) to 93.9(5)°, and O–I–O_{trans} is 180.0°.

There are four crystallization-independent silver atoms in **1**. Both Ag(1) and Ag(2) are four-coordinate, defined by two terminal oxygen atoms from two {MoO₆} octahedra of different polyoxoanions (Ag(1)–O = 2.571(14) and 2.582(14) Å and Ag(2)–O = 2.568(15) and 2.583(14) Å) and two central oxygen atoms from two polyoxoanions (Ag(1)–O = 2.176(10) and 2.184(10) Å and Ag(2)–O = 2.167(10) and 2.176(10) Å). The distance between the Ag(1) and Ag(2) atoms is 2.9312(14) Å, which is shorter than the sum of the van der Waals radii of two silver atoms (3.44 Å), suggesting significant silver(I)–silver(I) interactions. Both of the silver atoms form {Ag₂} linker groups that interconnect with the neighboring polyoxoanions to yield an unusual infinite anionic [Ag₂IMo₆O₂₄(H₂O)₄]³⁻ chain (Figure 3), which further demonstrates that the precursors in the reaction solution are not individual {Ag₂} and POM groups but are, most probably, {Ag(POM)Ag}-type synthons.²⁶ Both Ag-

(3) and Ag(4) are two-coordinate, coordinated by two nitrogen atoms from two different pyridine-4-carboxylic acid molecules (Ag(3)–N = 2.130(17) and 2.156(18) Å and Ag(4)–N = 2.146(16) and 2.158(16) Å). The proximity of the third oxygen atom, O(6), from the polyoxoanion to Ag(3) (Ag(3)–O(6) = 2.869 Å), which is shorter than the sum of the van der Waals radii of Ag and O (3.20 Å), implies weak binding and leads to the “T-shaped” coordination geometry around Ag(3). Similarly, there is a weak interaction between Ag(4) and O(5) from the polyoxoanion with a distance of 2.874 Å. The two adjacent silver–silver distances (Ag(3)–Ag(3) = 3.382 Å, Ag(3)–Ag(4) = 3.387 Å, and Ag(4)–Ag(4) = 3.390 Å) are shorter than the sum of the van der Waals radii of two silver atoms (3.44 Å).

There are two sodium atoms that have different coordination environments in **1**. Na(1) is seven-coordinate, defined by four carboxyl oxygen atoms from four pyridine-4-carboxylic acid molecules and three water molecules. The average Na(1)–O distance is 2.542 Å. Na(2), residing in a distorted octahedron geometry, is coordinated by four carboxyl oxygen atoms from four pyridine-4-carboxylic acid molecules and two water molecules. The average Na(2)–O distance is 2.509 Å. Each of the four crystallization-independent pyridine-4-carboxylic acid molecules acts as a tridentate ligand, coordinating to one silver atom and two sodium atoms (shown in Supporting Information Figure S1). Silver-pyridine-4-carboxylic acid coordination complexes are linked together by sodium atoms to form a cationic 2D polymer sheet (shown in Supporting Information Figure S2).

The most remarkable feature of compound **1** is that the new type of [IMo₆O₂₄(H₂O)₄]⁵⁻ cluster is utilized as the multidentate chelating ligand, coordinating to the {Ag₂} groups via the terminal and central oxygen atoms to yield an unprecedented 1D chain. To the best of our knowledge, no analogous extended structure consisting of this kind of POM has been reported in the literature. These chains further pillar the silver-organic coordination polymer sheets to form a 3D framework via weak Ag(3)–O and Ag(4)–O interactions (see Figure 4). It is notable that this kind of connection mode results in the formation of a fascinating channel along the *a*-axis, which is occupied by the lattice water molecules. The dimensions of the channel are ca. 8.7 × 3.3 Å (see Supporting Information Figure S3). Having studied the literature, we noticed that the exploitation of discrete POMs as the pillars to construct pillared 3D covalent or supramolecular frameworks has been successfully synthesized;²⁷ however, there are no examples of POM chain-pillared 3D frameworks to date.

It is also striking that the structure of compound **1** exhibits extensive hydrogen-bonding interactions among water molecules, pyridine-4-carboxylic acid molecules, and polyoxoanions. The typical hydrogen bonds are as follows: OW4···

(26) Abbas, H.; Pickering, A. L.; Long, D. L.; Kögerler, P.; Cronin, L. *Chem.–Eur. J.* **2005**, *11*, 1071.

(27) (a) Lü, J.; Shen, E. H.; Li, Y. G.; Xiao, D. R.; Wang, E. B.; Xu, L. *Cryst. Growth Des.* **2005**, *5*, 65. (b) Ishii, Y.; Takenaka, Y.; Konishi, K. *Angew. Chem., Int. Ed.* **2004**, *43*, 2702. (c) Li, Y. G.; Hao, N.; Wang, E. B.; Yuan, M.; Hu, C. W.; Hu, N. H.; Jia, H. Q. *Inorg. Chem.* **2003**, *42*, 2729.

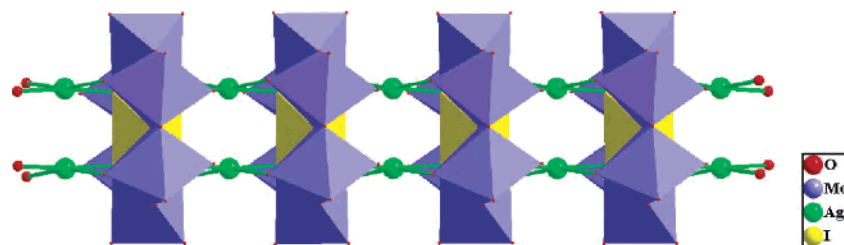


Figure 3. Polyhedral representation of the 1D anionic chain in **1**. Other atoms have been omitted for clarity.

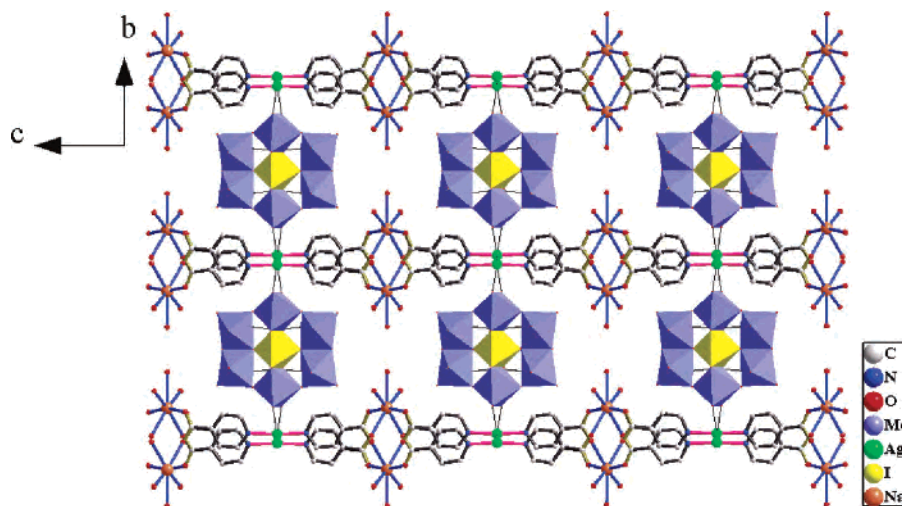


Figure 4. Polyhedral and ball-stick representation of the 3D supramolecular framework of **1** via weak Ag–O interactions running along the *a*-axis. Lattice water molecules have been omitted for clarity.

O10 = 2.909(2) Å, OW4...OW13 = 2.80(3) Å, OW3...O4 = 2.937(2) Å, OW3...OW12 = 2.78(2) Å, OW11...O33 = 2.772(4) Å, C1...O7 = 3.364(4) Å, and C17...O13 = 3.315(2) Å (shown in Supporting Information Table S1). It is believed that the extensive hydrogen-bonding interactions play an important role in stabilizing the 3D supramolecular structure (Supporting Information Figure S4).

Crystal Structure of 2. Single-crystal X-ray diffraction analysis shows that compound **2** is made up of $[\text{IMo}_6\text{O}_{24}]^{5-}$ clusters, trinuclear Ag-pyridine-3-carboxylic acid coordination complexes, sodium ions, and lattice water molecules. The $[\text{IMo}_6\text{O}_{24}]^{5-}$ cluster has an A-type Anderson structure in which six $\{\text{MoO}_6\}$ octahedra arrange hexagonally around the central $\{\text{IO}_6\}$ octahedron (see Figure 5). According to the way the oxygen atoms are coordinated, five kinds of oxygen atoms exist in the cluster: terminal oxygen Ot, terminal oxygen Ot₁ linked to Ag⁺, terminal oxygen Ot₂ linked to Na⁺, double-bridging oxygen Ob, and central oxygen Oc. Thus, the Mo–O distances can be grouped into five sets: Mo–Ot = 1.709(6) and 1.711(5) Å, Mo–Ot₁ = 1.703(5) and 1.711(5) Å, Mo–Ot₂ = 1.703(5) and 1.716(4) Å, Mo–Ob = 1.916(5)–1.941(5) Å, and Mo–Oc = 2.298(4)–2.359(5) Å. The central I–Oc distances vary from 1.876(5) to 1.887(4) Å. The bond angles of O–I–O_{cis} range from 86.6(2) to 93.4(2)°, and O–I–O_{trans} is 180.0°.

There are two crystallization-independent silver atoms. Ag(1) is four-coordinate, defined by two terminal oxygen atoms from two $[\text{IMo}_6\text{O}_{24}]^{5-}$ units (Ag(1)–O = 2.586(5) and 2.631(5) Å) and two nitrogen atoms from two pyridine-3-carboxylic acid molecules (Ag(1)–N = 2.178(6) and 2.191-

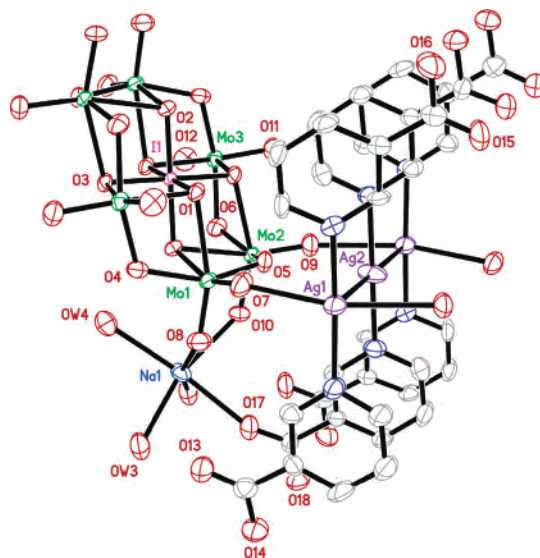


Figure 5. ORTEP drawing of **2** with thermal ellipsoids at 50% probability. Other atoms have been omitted for clarity.

(6) Å). Ag(2) is coordinated in a linear geometry by two nitrogen atoms from two pyridine-3-carboxylic acid molecules (Ag(2)–N = 2.153(6) Å). A pair of Ag(1) atoms is linked by the Ag(2) atom via silver–silver bonds, resulting in a trinuclear silver(I) cluster. The distance (3.242 Å) between Ag(1) and Ag(2) is shorter than the sum of the van der Waals radii of two silver atoms (3.44 Å). There are three crystallographically independent pyridine-3-carboxylic acid molecules. Two pyridine-3-carboxylic acid molecules act as monodentate ligands, coordinating to a Ag(1) atom, whereas

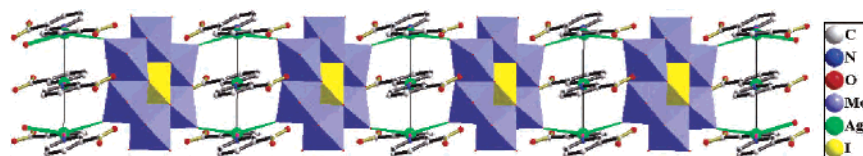


Figure 6. View of the 1D hybrid chain in **2**. Sodium atoms and water molecules have been omitted for clarity.

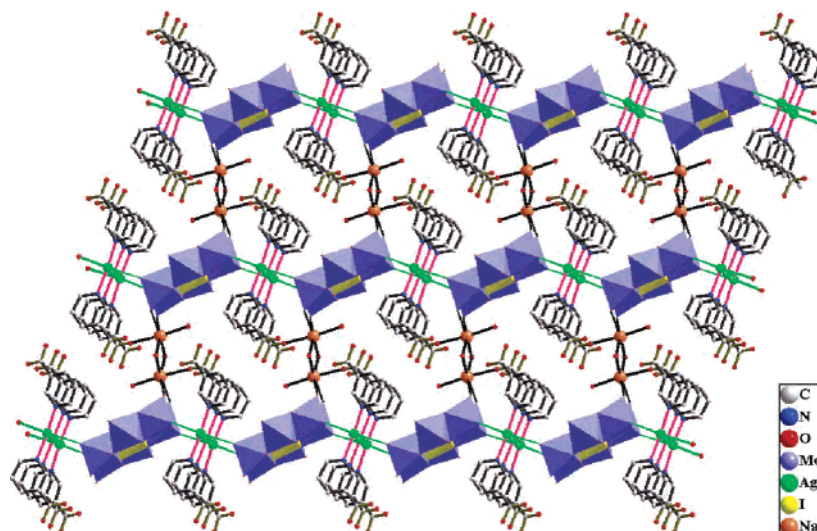


Figure 7. View of the 2D hybrid network in **2**. Lattice water molecules have been omitted for clarity.

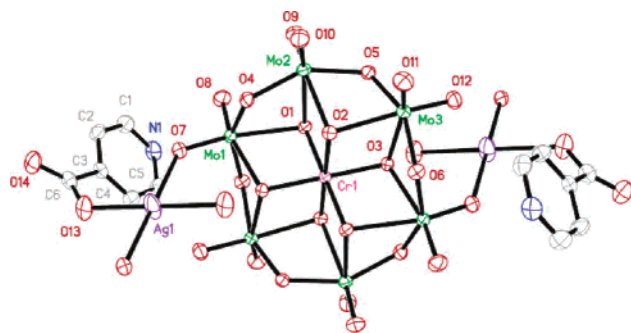


Figure 8. ORTEP drawing of **3** with thermal ellipsoids at 50% probability. Other atoms have been omitted for clarity.

another one acts as a bidentate ligand, coordinating to a Ag(2) and a sodium atom. The crystallographically unique Na atom links to two terminal oxygen atoms from one $[\text{Mo}_6\text{O}_{24}]^{5-}$ unit, one carboxyl oxygen atom from the pyridine-3-carboxylic acid molecule coordinated to Ag(2), and three water molecules to finish its octahedral coordination environment. The average Na–O bond length is 2.398 Å. Two water molecules bridge two adjacent Na atoms to form a sodium dimer.

In the structure of **2**, trinuclear Ag-pyridine-3-carboxylic acid fragments connect the $[\text{Mo}_6\text{O}_{24}]^{5-}$ polyoxoanions to construct a 1D chain (see Figure 6). The infinite chains are further held together by sodium dimers to yield a planar sheet (Figure 7). A significant feature is that the planar sheets are stacked to give a 3D supramolecular framework with 1D channels of nearly 6.8×5.4 Å along the *a*-axis (see Supporting Information Figure S5). Lattice water molecules are located in the channels and form multipoint hydrogen bonds with the nearest lattice water molecules, coordinated water molecules, and oxygen atoms of polyoxoanions (shown

in Supporting Information Table S2). Obviously, these hydrogen-bonding interactions play an important role in the formation of the 3D supramolecular framework. To the best of our knowledge, compound **2** represents the first example of a 2D inorganic–organic hybrid framework containing the Anderson-type polyoxoanions and silver–organic coordination complexes.

The pillared 3D supramolecular framework in **1** and the 2D inorganic–organic hybrid framework in **2** are all synthesized from the A-type Anderson cluster. The obvious structural difference between compounds **1** and **2** is due to the introduction of different organic molecules. This has further demonstrated that organic molecules can profoundly influence the framework structure because of their different coordination modes.

Crystal Structure of 3. Single-crystal X-ray structural analysis shows that the structure of **3** is a new 1D chainlike polymer which consists of $[\text{Cr}(\text{OH})_6\text{Mo}_6\text{O}_{18}]^{3-}$ building blocks, Ag-pyridine-4-carboxylic acid coordination complexes, free pyridine-4-carboxylic acid molecules, and lattice water molecules. The $[\text{Cr}(\text{OH})_6\text{Mo}_6\text{O}_{18}]^{3-}$ cluster has a B-type Anderson structure in which each heteroatom Cr forms an octahedral complex of six OH groups. According to the way the oxygen atoms are coordinated, four kinds of oxygen atoms exist in the cluster: terminal oxygen Ot, terminal oxygen Ot' linked to Ag^+ , double-bridging oxygen Ob, and central oxygen Oc. Thus, the Mo–O distances can be grouped into four sets: Mo–Ot = 1.698(2)–1.722(2) Å, Mo–Ot' = 1.720(2) Å, Mo–Ob = 1.922(2)–1.9657(19) Å, and Mo–Oc = 2.228(2)–2.327(2) Å. The central Cr–Oc distances vary from 1.9556(18) to 1.980(2) Å. The bond angles of O–Cr–O_{cis} range from 82.45(9) to 97.55(9)°, and O–Cr–O_{trans} is 180.0°.

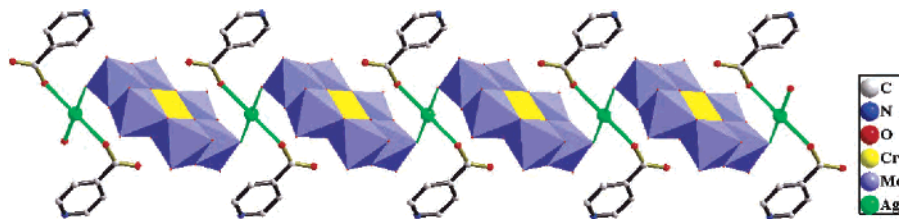


Figure 9. View of the 1D hybrid chain in **3**. Free organic molecules and water molecules have been omitted for clarity.

In the structure of **3**, crystallographically unique silver(I) is four-coordinate, completed by two oxygen atoms from two $[\text{Cr}(\text{OH})_6\text{Mo}_6\text{O}_{18}]^{3-}$ polyoxoanions and two carboxyl oxygen atoms from two pyridine-4-carboxylic acid molecules (see Figure 8). The average Ag–O bond length is 2.422 Å. Each pyridine-4-carboxylic acid molecule acts as a monodentate ligand by utilizing its carboxylate group to coordinate to a silver atom.

These Ag-pyridine-4-carboxylic acid coordination complexes link $[\text{Cr}(\text{OH})_6\text{Mo}_6\text{O}_{18}]^{3-}$ building blocks together to form 1D chainlike polymers (see Figure 9), which are further held together to form an unusual supramolecular 2D layer (Supporting Information Figure S5) via hydrogen bonds between the coordinated pyridine-4-carboxylic acid molecules and the hydroxides of the central $\text{Cr}(\text{OH})_6$ moiety, such as $\text{C1}\cdots\text{O8} = 3.043(5)$ Å and $\text{N1}\cdots\text{O8} = 2.984(3)$ Å. There also exist extensive hydrogen bonds among free organic molecules, water molecules, and polyoxoanions (see Supporting Information Figure S7). The representative hydrogen bonds are as follows: $\text{N1}\cdots\text{O15} = 2.797(4)$ Å, $\text{N2}\cdots\text{O5} = 2.661(3)$ Å, $\text{O1}\cdots\text{O14} = 2.768(3)$ Å, $\text{O2}\cdots\text{OW2} = 2.665(3)$ Å, $\text{C8}\cdots\text{O9} = 3.052(6)$ Å, $\text{C11}\cdots\text{O12} = 3.330(8)$ Å, and $\text{OW1}\cdots\text{OW2} = 2.817(8)$ Å (shown in Supporting Information Table S3).

When the basic building block is changed from an A-type to a B-type Anderson structure in the presence of pyridine-4-carboxylic acid molecules, that is, the same organic ligand as used in compound **1**, the structure of the obtained compound **3** is completely different from that of compound **1**. We also have experimented with the B-type Anderson structure as the cluster in the presence of pyridine-3-carboxylic acid molecules; however, no compounds containing silver ions or their coordination complexes were obtained. This confirms that the POM building blocks perform a very important role in constructing the extended architectures because they possess different negative charges and different reaction pH values.

The bond valence sum calculations²⁸ indicate that all I sites are in the +7 oxidation state, all Ag sites and Na sites are in the +1 oxidation state, and all Mo sites are in the +6 oxidation state in compounds **1** and **2**. In compound **3**, all Cr sites are in the +3 oxidation state, all Ag sites are in the +1 oxidation state, and all Mo sites are in the +6 oxidation.

XPS Spectroscopy. The XPS spectra of compound **1** in the energy regions of Mo 3d, Ag 3d, and Na 1s show peaks at 232.5, 368.5, and 1072.1 eV, respectively, attributable to Mo^{6+} , Ag^+ , and Na^+ . The XPS spectra of compound **2** in

the energy regions of Mo 3d, Ag 3d, and Na 1s show peaks at 232.2, 368.2, and 1071.2 eV, respectively, attributable to Mo^{6+} , Ag^+ , and Na^+ . The XPS spectra of compound **3** in the energy regions of Mo 3d and Ag 3d show peaks at 232.0 and 368.0 eV, respectively, attributable to Mo^{6+} and Ag^+ (see Supporting Information Figure S8a–c). These results further confirm the composition of compounds **1**, **2**, and **3**.

ESR Spectroscopy. ESR studies have been undertaken to elucidate the electronic properties of the Cr^{3+} in compound **3**. The ESR spectrum of compound **3** was recorded at room temperature on a polycrystalline powder sample (shown in Supporting Information Figure S9). The effective *g*-values of ≈ 1.97 , 3.26, and 3.92 are typical of an electronic spin, $S = 3/2$, with moderately large zero field splitting and small rhombicity.²⁹ These spectral features compare well to those reported in the literature for the Cr^{3+} spin systems.³⁰

FT-IR Spectroscopy. In the IR spectrum of compound **1**, the characteristic peaks at 942, 904, 889, 764, 698, 624, 476, and 417 cm^{-1} are attributed to the $[\text{IMo}_6\text{O}_{24}(\text{H}_2\text{O})_4]^{5-}$ polyoxoanion and the characteristic bands at 3528, 3452, 3351, 1963, 1714, 1607, 1548, 1413, 1390, 1337, 1232, and 1215 cm^{-1} can be regarded as features of the pyridine-4-carboxylic acid molecule. In the IR spectrum of compound **2**, the characteristic peaks at 941, 905, 813, 745, 693, 681, 622, and 470 cm^{-1} demonstrate that $[\text{IMo}_6\text{O}_{24}]^{5-}$ is an Anderson structure and characteristic bands in the region from 3539 to 1202 cm^{-1} can be regarded as features of the pyridine-3-carboxylic acid molecule. In the IR spectrum of compound **3**, the characteristic peaks at 942, 922, 907, 886, 830, 767, 757, 680, 642, 561, 537, and 412 cm^{-1} are attributed to the $[\text{Cr}(\text{OH})_6\text{Mo}_6\text{O}_{18}]^{3-}$ polyoxoanion and the characteristic bands in the region from 3563 to 1223 cm^{-1} can be regarded as features of the pyridine-4-carboxylic acid molecule (Supporting Information Figure S10a–c).

TG Analyses. The thermal gravimetric (TG) curve of **1** is shown in Supporting Information Figure S11a. It shows a total weight loss of 39.52% in the range of 40–781 °C, which agrees with the calculated value of 40.70%. The weight loss of 11.44% at 40–169 °C corresponds to the loss of all noncoordinated and coordinated water molecules (calcd 11.78%). The weight loss of 28.08% at 171–781 °C arises from the decomposition of pyridine-4-carboxylic acid molecules, iodine molecules, and partial oxygen molecules (calcd 28.92%).

(29) Jacquamet, L. L.; Sun, Y. J.; Hatfield, J.; Gu, W. W.; Cramer, S. P.; Crowder, M. W.; Lorigan, G. A.; Vincent, J. B.; Latour, J. M. *J. Am. Chem. Soc.* **2003**, *125*, 774.

(30) (a) Shaham, N.; Cohen, H.; Meyerstein, D.; Bill, E. *J. Chem. Soc., Dalton Trans.* **2000**, 3082. (b) Casellato, U.; Graziani, R.; Bonomo, R. P.; Bilio, A. J. D. *J. Chem. Soc., Dalton Trans.* **1991**, 23.

(28) Brown, I. D.; Altermatt, D. *Acta Crystallogr., Sect. B* **1985**, *41*, 244.

The TG curve of compound **2** exhibits three continuous weight loss stages in the range of 36–791 °C (Supporting Information Figure S11b), corresponding to the release of all water molecules, pyridine-3-carboxylic acid molecules, iodine molecules, and partial oxygen molecules. The whole weight loss (47.03%) is in good agreement with the calculated value (46.35%).

The TG curve of **3** is shown in Supporting Information Figure S11c. It shows a total weight loss of 35.67% in the range of 77–533 °C, which agrees with the calculated value of 36.53%. The weight loss of 4.02% at 77–166 °C corresponds to the loss of lattice water molecules (calcd 4.26%). The weight loss of 31.65% at 187–533 °C arises from the loss of all composed water molecules and the decomposition of organic moieties (calcd 32.27%).

Conclusions

In summary, the success in synthesizing compounds **1**, **2**, and **3** provides novel examples of the utilities of presynthesized Anderson clusters as precursors and silver ions as bridges in the presence of organic ligands for constructing extended solid-state materials. The structure of **1** possesses a 3D supramolecular framework composed of metal-organic polymer layers pillared by the silver polyoxometalate chains.

The present work may supply a potential method for forming other related pillared structures via alterations to POM building blocks or transition metals. Compound **2**, with 2D hybrid networks, and compound **3**, featuring 1D hybrid chains, were obtained when we changed the organic ligand from the pyridine-4-carboxylic acid in **1** to the pyridine-3-carboxylic acid in **2** or the building block from A-type Anderson in **1** to B-type Anderson in **3** under similar reaction conditions. This underpins the ability of the organic molecules and the basic building units to influence profoundly the structure of synthesized products and to direct their formation with particular structural and physical properties. This approach is expected to be effective for the construction of further novel high-dimensional POM frameworks, and more investigations are underway.

Acknowledgment. The authors thank the National Natural Science Foundation of China (20371011) for financial support.

Supporting Information Available: X-ray crystallographic files for compounds **1**, **2**, and **3** in CIF format and additional figures and tables. This material is available free of charge via the Internet at <http://pubs.acs.org>.

IC050636X